Woolitmus: An Approach to Minimize E–waste using Wool-Based Wearable Sensor for Sweat pH Detection

Shruti Ghadge, Aditya Marathe, Ravindra Adivarekar and Sandeep More**

Institute of Chemical Technology, Nathalal Parekh Marg, Matunga East, Mumbai,
Maharashtra, India 400019
E-mail: sp.more@ictmumbai.edu.in

Keywords: Wearable sensors, Pyranine, Medical Textiles, Sweat patches, E–waste

Abstract:

This study introduces ***"Woolitmus"*** a textile-based wearable sweat pH indicator developed using pyranine, also known as HPTS (8-Hydroxypyrene-1,3,6-trisulfonic acid) and naturally occurring wool as substrate. Sweat pH analysis is crucial for monitoring health conditions associated with pH imbalance. The sensor exhibits pH responsiveness under both visible and UV light, offering potential as a real-time sweat patch for pH monitoring. The interaction of pyranine with wool substrate is detailed, elucidating the mechanism behind the pH sensitivity backed up by photophysical characterizations. Stability and reversibility tests also confirm the sensor's robustness and performance. The reported sensor also can simultaneously collect and detect pH levels without support of any additional accessories like electrodes, display, etc. It also offers sensitivity, real-time response, and non-invasive detection. But more importantly it stands out for its biodegradability, reusability, zero e-waste, and biocompatibility of the substrate. The wool fabric-based pH sensor holds promising applications, including health monitoring and lifestyle management.

1. Introduction

Sweat pH analysis is essential for detecting health issues related to pH balance disruption. Normal sweat pH ranges from 4.5 to 7, but deviations indicate shifts toward acidity or alkalinity. Conditions like cystic fibrosis are evident through sweat's pH, which can approach to 9 due to bicarbonate imbalance. Monitoring sweat pH changes can provide early alerts for such concerns.[1–3] Sweat pH also helps spot infections in wounds. Altered sweat pH (7 to 8.5) caused by bacteria and enzymes signals infected wounds, aiding in tracking the body's response. Moreover, sweat pH variations impact wound healing assessment. Changes during healing stages offer insights into treatment effectiveness, non-invasively gauging the body's reaction.[4,5] Dermatological health benefits from sweat pH analysis too. Skin issues like irritant contact dermatitis, atopic dermatitis, and acne correlate with sweat pH. Analyzing sweat composition aids diagnosis and monitoring, offering a non-invasive tool for dermatologists.[6] The connection between sweat pH and glucose levels offers further benefits.[7] Sweat pH reveals physical exertion levels and dehydration signs. Evaluating sweat pH changes distinguishes exercise from dehydration.[8–12] Hence, sweat pH analysis is versatile for diagnosing diverse health conditions. From metabolic disorders to infections and skin ailments, sweat pH provides insights into health and responses to internal and external factors.

Various pH sensor categories have been explored, including ionic liquid-based sensors[13–16] metal complex-based sensors[17,18] and carbon electrode, graphene-based sensors.[19,20] However, each category presents certain limitations in the terms of recyclability, flexibility and compatibility. For example, liquid-based sensors face usage cycle constraints, while metal complex sensors excel in specificity and sensitivity but lack flexibility. Carbon and graphene electrode sensors offer specificity and responsiveness but are challenged by flexibility and compatibility issues. A common challenge with these sensors is the requirement for extra accessories to convert observed changes into quantified or readable data. Furthermore, the process of sweat collection and detection is not concurrent, necessitating separate device for each step. The inclusion of additional components and separate devices in wearables contributes to electronic waste. As these devices become outdated or are replaced, they compound the environmental challenge of e-waste disposal. while each type of sensor offers unique advantages, they all share common challenges related to usage, interpretation of data, and waste generation, which need to be addressed for the continued advancement and sustainability of wearable technology. Researchers have also explored integrating these sensors directly onto textile substrates.[3,21–23] Textile substrates have benefits such as flexibility, biocompatibility, biodegradability and aiding sweat flow to the device. However, directly integrating sensors onto textiles superficially doesn't fully solve challenges like skin irritation, limited permeability, and user-unfriendly arrangements.

Considering these factors, there's a demand for sensors that harmonize with the human body, enabling simultaneous collection and detection. These sensors should offer sensitivity, real-time response, and non-destructive detection. A promising approach involves directly impregnating sensory material into textile substrates with required exposure to the stimuli. In existing literature, curcumin-based sensors have been developed, directly printed onto textile substrates.[22]These sensors exhibit strong responsiveness and biocompatibility but presents challenges like poor washing fastness and concern of durability. After careful consideration of all aspects, we introduced pyranine (8-Hydroxypyrene-1,3,6-trisulphonic acid) based sweat pH sensor using wool fabric as natural biodegradable substrate. The bond formation of pyranine molecules occurs through the sharing or transfer of electrons between functional groups of wool through hydrogen bonding and acid-base interactions leading to the creation of stable chemical bonds. This approach establishes pH sensor that combines colorimetric and fluorometric methods.

This pyranine based sensor addresses several challenges observed in previously mentioned pH sensors. By utilizing pyranine, a well-established pH-responsive and non-toxic organic dye[24–26] we could get real-time response, non-destructive detection, biocompatibility, sensitivity, and simultaneous sweat collection and pH detection. The application on wool fabric not only capitalizes on its attributes but also ensures comfort and compatibility with the human body, similar to wearing ordinary clothing. This advancement offers improved durability and reversibility, enhancing its practicality and application potential.

2. Results and discussion:

2.1. Interaction of pyranine with wool substrate -Acid dyeing on wool

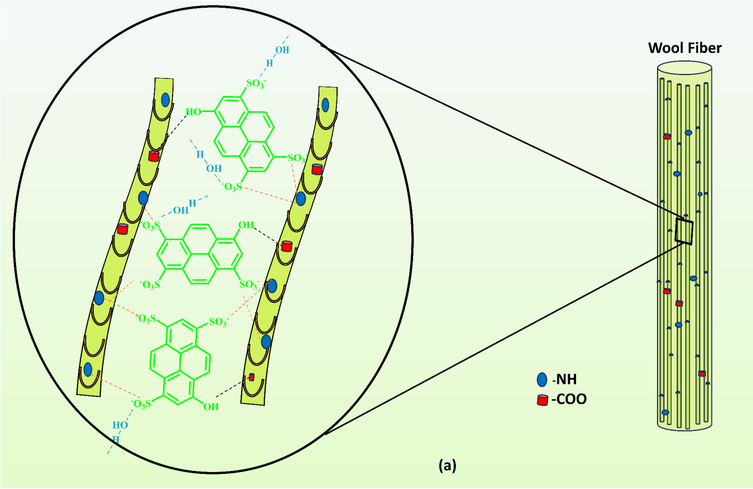

Figure 1:*Schematic representation illustrating dye molecules adhering to substrate fibres through different types of interactions.*

Pyranine has a stable molecular structure with fused aromatic rings made of carbon atoms bonded by covalent bonds. It also contains functional groups like hydroxyl (-OH) and sulfonic acid (-SO_3H), enabling it to engage in different chemical reactions, such as hydrogen bonding and acid-base interactions. Many acid dyes commonly used for dyeing wool and other protein fibers share similar properties, making them suitable for application on wool fabric. The way pyranine interacts with wool is comparable to other acid dyes.

In protein fibers like wool, silk, and nylon, there are amino and carboxyl groups. When the environment is slightly acidic, around pH 5, these groups become ionized, transforming into NH_3^+ and $COO^{-.}$ The sulphonyl groups on pyranine interact with the NH_3^+ ions, resulting in ionic interactions. As mentioned, pyranine can form hydrogen bonds and also experiences van der waals forces of attraction which also contributes to the chemical bonding of pyranine with substrate. Ammonium groups and fiber's amorphous parts are crucial. Amorphous regions ease dye penetration; more ammonium groups intensify interaction with anions in dyes, improving dyeing uniformity and fastness. Wool stands out among protein fibers as a substrate for pyranine. This is because wool has significantly more ammonium groups (20 times more than nylon and 5 times more than silk).[27] and its amorphous nature helps with dye absorption and diffusion. These features of wool uniquely promote the acceptance of pyranine, resulting in uniform and long-lasting coloration.

2.2 Mechanism of pH responsiveness:

The emission of pyranine is linked to its Pka values, with ground state Pka around 7.3 – 7.7 and excited-state Pka* around 0.4 – 1.3.[24,28–30] This creates a dual pH-sensing mechanism. pH above the pKa (proton is not tightly held), pyranine exists mainly as RO^-, emitting RO^{-*} at around 510 nm upon excitation. Conversely, at pH below the pKa (proton tightly held), pyranine is mostly in the ROH form, producing ROH* upon excitation. The excited-state proton transfer (ESPT) process then converts ROH* to RO^-* with emission at ~510 nm. This leads to different steady-state excitation spectra at pH above and below the pKa, indicating distinct pathways to reach RO^-*. Above the pKa, RO^-* emission primarily comes from RO^-, while below the pKa, it mainly comes from ROH. When using pyranine as a fluorescent pH indicator, one can either monitor RO^-* emission with increasing pH during RO^- excitation, or measure the fluorescence excitation spectrum at the emission. The key sensing element in pyranine is its hydroxyl (OH) group. Even though ionic interactions with wool fibers occur during dyeing, they do not significantly impact pH sensing. Thus, the wool fabric maintains consistent pH-sensing behavior. Post-dyeing pH sensitivity remains constant, but it slightly affects pyranine's interaction with wool. In acidic conditions, pyranine strongly adheres to wool, while in strong basic conditions, slight leaching occurs.

The fabric's pH-sensing capabilities were investigated in both its ground and excited states. As a ground state pH indicator, the fabric exhibits a reddish hue under acidic conditions, while it appears yellowish-green (fluorescent) in the basic range. This color change is directly proportional to its interaction with the substrate. In acidic environments, there is a strong ionic interaction between wool and pyranine. Conversely, in basic medium, the interaction between pyranine and wool weakens, leading to the partial release of pyranine from the interaction. A chromaticity diagram in the CIE 1976 color space was generated for samples at acidic, neutral and basic conditions utilizing reflectance values recorded with a CCM instrument under D-65 light. This diagram visually depicts the distribution of hue and saturation to an observer under D-65 light, thereby highlighting the potential of the dyed fabric as a ground state pH indicator. Notably, the color coordinates of the dyed fabric closely align with those of pH 7, indicating that the dyed fabric can serve directly as a reference.

The distinct characteristics of pyranine remain unchanged in our prepared sample, leading to its unaltered behavior in its excited state as well. So, Under UV light, a distinct tripartite pattern is observed resembling the Acid, Neutral, and Base zones. This pattern is showing the significant shifts in fluorescence. The Acidic zone shifts from blue to cyan fluorescence, while the middle zone maintains the fabric's color but with slightly enhanced fluorescence. The Basic

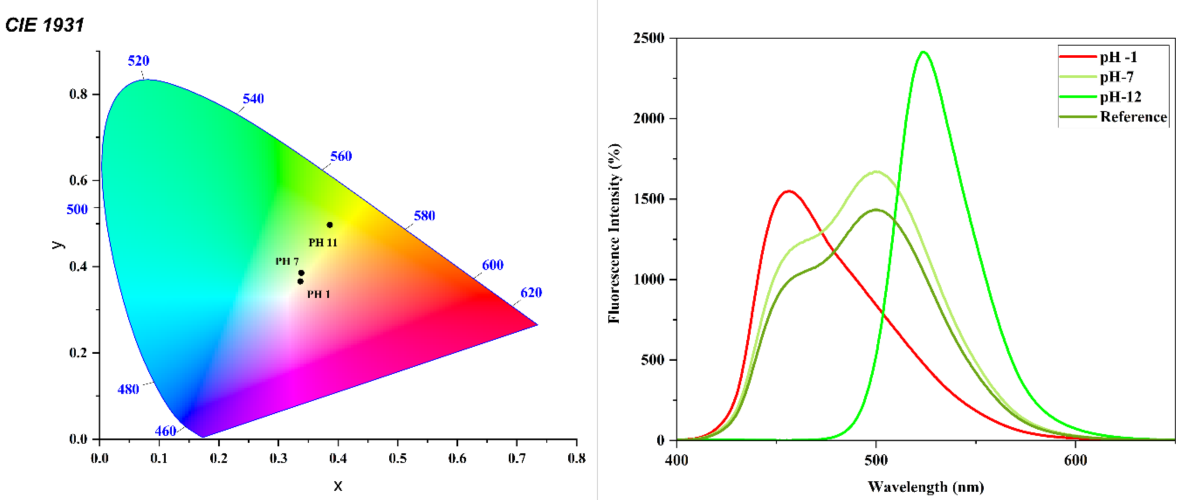

***Figure 3**: a) CIE 1931 chromaticity diagram of pH 1,7 and 11 (b) Emission Spectra Illustrating Emission Changes at Varying pH Values of 1,7and 12 along with reference dyed fabric sample.*

zone exhibits intense green-yellow fluorescence with the highest luminosity. Validation is provided through emission which confirms the presence of three distinct zones. Emission in the acidic zone occurs around 426 nm, while the basic zone it emits around 525 nm. Interestingly, emission spectra from the middle zone show characteristics of both acidic and basic profiles that can be attributed to formation of hybrid profile. This observations underscores germinate pair formation possibility[31,32]. This observations underscores wool's pH detection capability, shedding light on pyranine's behavior in an excited state.

Emission in Acidic, Neutral, and Basic zones is ruled by interconversions of ROH and RO^- states across the pH variations. Our findings match the Förster cycle framework[33]. When the compound is protonated (ROH state), it emits light at 426 nm, and when deprotonated (RO– state), it emits at 525 nm. This confirms our samples follow established patterns. However, In the middle zone, pyranine's oxygen part forms pairs with ions from the buffer solution. When shifting towards basicity, the hydroxyl group partly separates, and when shifting towards acidity, it partly attaches. This middle state shows traits of both peaks, confirming pyranine's complex pH-dependent behavior in different conditions and proving its versatility in our sample.

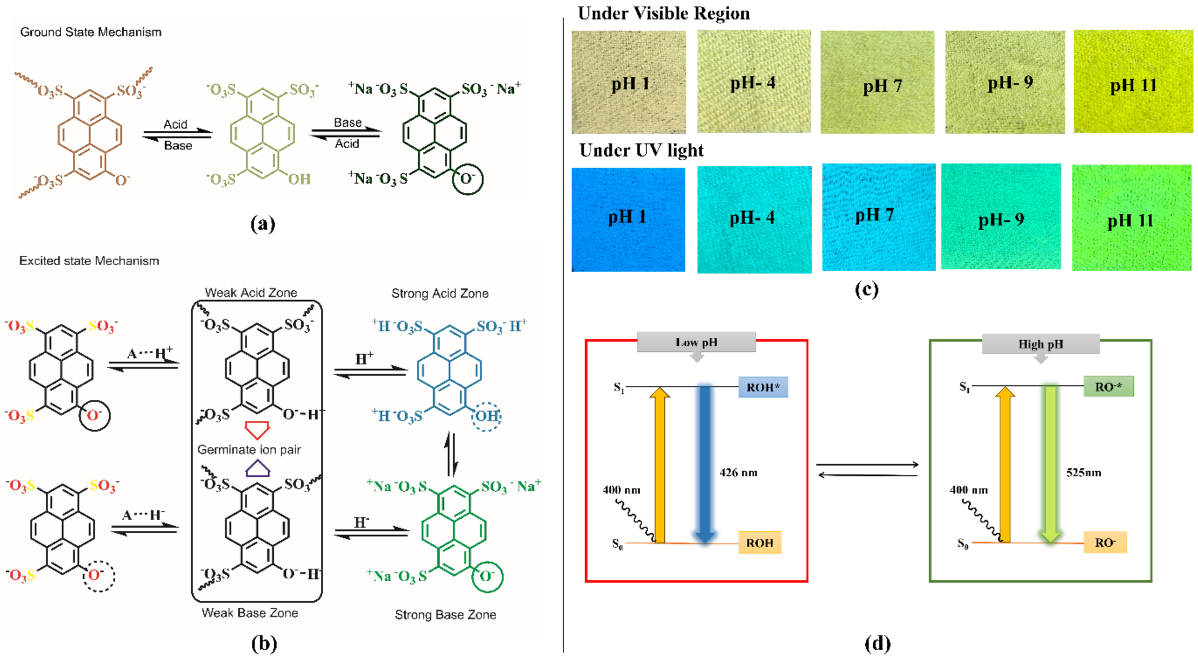

Figure 2:*(a) Ground State Mechanism for pH Sensing (b) Excited state pH sensing Mechanism (c) Different pH treated dyed wool fabric under visible and UV light (d) Illustration of pH sensing mechanism on the basis of energy levels in ground and excited state.*

FTIR analysis **(Figure S2)** indicates the presence of tertiary alcohol (1036–1040 cm^{-1}) and sulphonyl group (1171–1182 cm^{-1}) in the dyed fabric, as well as in the acid and base-treated samples. The tertiary alcohol groups might play a role in facilitating the presence of pyranine on the fabric. Additionally, the broadening of OH^{-} bands (3451–3454 cm^{-1}) in the base-treated same implies a potential interaction between the base and pyranine molecules, leading to the release of pyranine from the fabric. The SEM analysis **(Figure S3)**, despite not showing any surface deposition of dye, suggests that the dye is effectively trapped within the wool fibers. This could be due to interactions and ionic bonding, which led to the incorporation of the dye molecules into the fabric structure.

Shade %	Dry rub fastness	Wet rub fastness	Wash Fastness
5%	5	5	5
Rating: 1 –Poor ,2- Fair,3- Good,4 –Very good 5- Excellent			

Table 1: Washing and rubbing (Dry and Wet) fastness rating

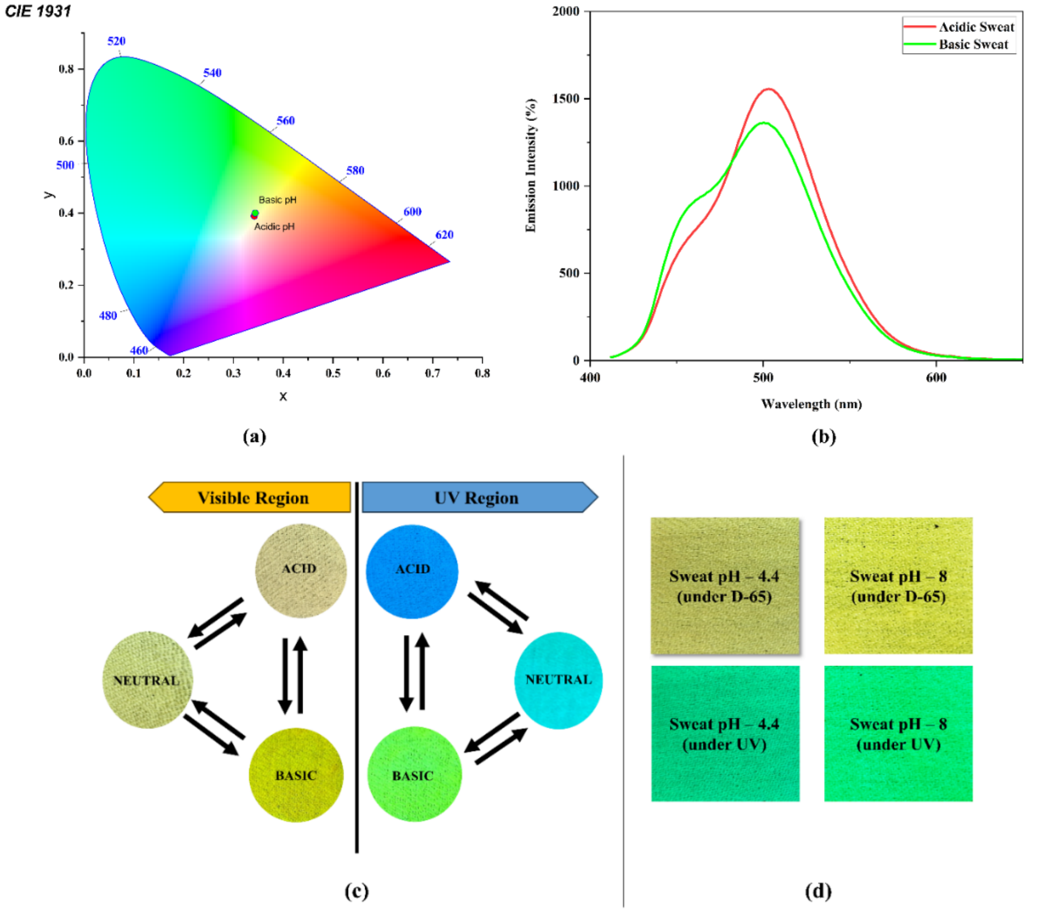

Figure 4: *(a) CIE colour space chromaticity diagram of both acidic and basic artificial Sweat (b) Emission Spectra for Acidic Sweat and Basic Sweat pH (c) Exploring Reversibility through Combinations (d) Wool fabric samples after treating with artificial sweats*

The stability analysis of the samples was conducted to assess their resistance against rubbing and washing, with readings documented as per the standard procedures out-lined in the experimental section. The readings obtained **(Table:1)** shows both the rubbing and washing resistance tests offers excellent durability and robustness of the samples, and have ability to withstand the challenges posed by rubbing and repeated washing.

The prepared sample can change color back and forth between acidic ↔ basic, acidic ↔ neutral, and basic ↔ neutral conditions under both UV and visible light, as seen in Figure 4(b). We analyzed its performance in artificial sweat (Table 2) to evaluate its potential as a sweat analyzer. By recording CIE 1976 and emission spectra, we tested its effectiveness as a real-time sweat patch monitor. The results mirrored those from the buffer solution tests, suggesting 'Woolitmus' holds promise for this application.

2.3 Application:

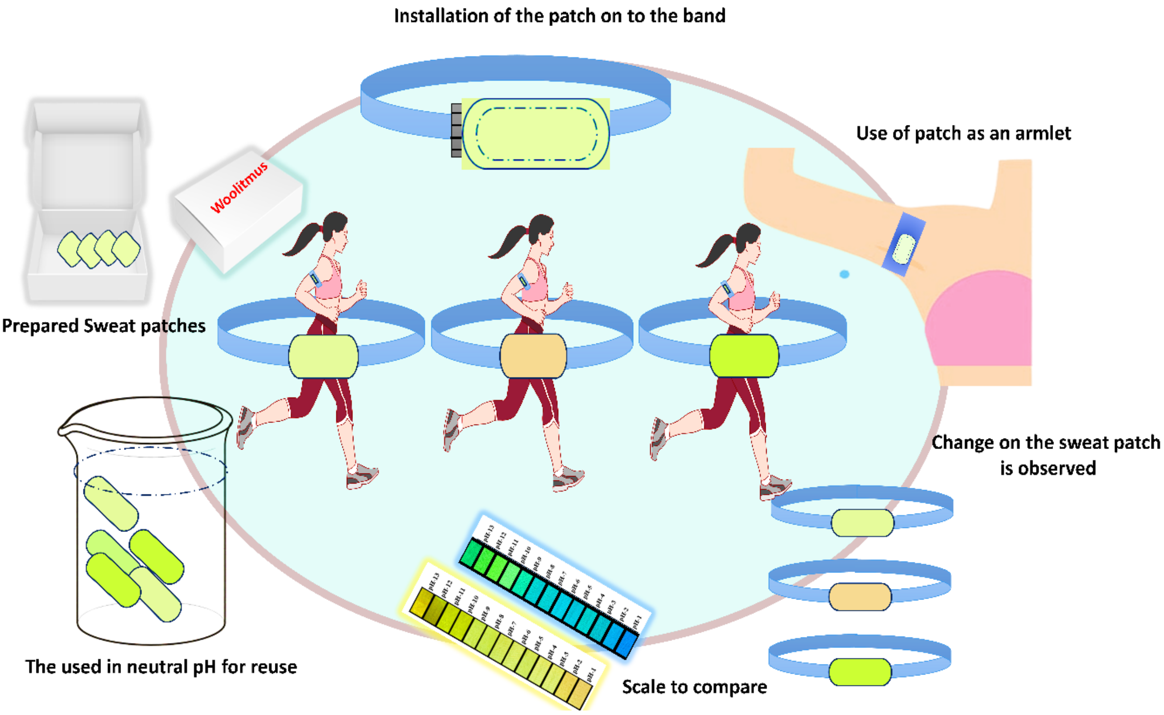

***Figure 5**: Illustration of representing proposed sweat patch along with the construction, procedure of applications and reusability; Ideal for infants with cystic fibrosis or sweat pH issues. Continuous, comfortable monitoring.*

https://doi.org/10.26434/chemrxiv-2024-ltkxm-v2 **ORCID:** https://orcid.org/0000-0002-4187-7007

The illustration depicts a pH-sensitive patch called Woolitmus, designed for real-time applications like health monitoring and fitness tracking. Woolitmus's construction and applications are outlined in Figure 5, highlighting its potential impact. One noteworthy aspect is its reversibility, which allows it to be reused after being immersed in a neutral solution. This feature significantly reduces electronic waste generated by wearables and enhances the economic feasibility of continuous monitoring. Users can compare the patch's color change to a reference or provided color scale to assess sweat pH in real-time. Detecting unusual pH changes can indicate underlying health conditions, prompting the need for medical attention or early intervention. With further advancements, this concept holds promise for enhancing healthcare and wellness on a broader scale, potentially revolutionizing how individuals monitor and manage their health and fitness levels.

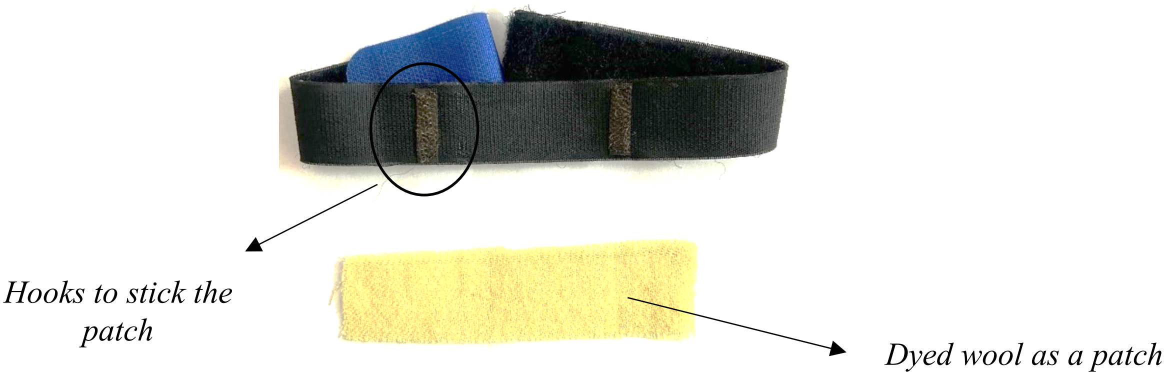

Figure 6: *Prototype of proposed sweat sensor*

4. Experimental section:

4.1 Acid Dyeing of wool using Pyranine:

For the fabrication of this textile-based sensor simply acid dyeing of wool in open bath was carried out. Various stages of dyeing procedure along with the temperature to be maintained is mentioned in (Figure S4). Referencing the same at the start by calculating material to liquor ratio (MLR)1:20; liquor and the fabric was inserted in the pot. After the time interval of 5 minutes first addition of 2 % formic acid and 5% galubers salt (A) was carried out. Following another 5 minutes pyranine was added according to shade percentage (B) addition was performed in the same pot. Afterwards again in the interval of 5 minutes increased the temperature to 100°C. After processing the fabric for 30-45 minutes in the same bath insertion of 2% Formic acid in combination with 2% sulphuric acid was added (C) to provide acidic environment for the electrostatic interaction and fixation of the pyranine on wool. Further wool fabric was processed for 30 more minutes in the same acidic environment before the washing with non-ionic soap and air drying was carried out.

4.2 Characterization:

Scanning electron microscopy is used to analyze the surface morphology of the fabric to confirm the dyeing and not the surface deposition. Similarly, fourier transform infra-red (FT-IR) spectra of fabric (Dyed wool reference, fabric treated with pH 1 and pH 12) was performed on Shimadzu FTIR 8400S to detect the change in functional groups due to ionic environment. Prepared fabric-based sensor shows the change in UV and visible light both. To interpret the behavior in UV region, emission spectra of the sample recorded using JASCO 6000 fluorescence spectroscopy. To prove the changes with pH in visible light, CIE chromaticity diagram was plotted using colorfast color matching machine.

4.3 pH colorimetric sensing test:

To prove the creditability of the prepared dyed wool fabric as pH sensor, the dyed fabric was checked against the viable pH range. To check the change, the pH solution was poured into the small beaker and the strip of the fabric was half dipped into the solution for one minute. As mentioned, the change occurs is detected and interpreted in UV and visible light using emission spectra and CIE color space values respectively. Investigate sample reversibility by testing against pH 1, 7, and 12. Immerse samples in corresponding buffers for one minute based on reversibility sequence (e.g., acid ↔ base, acid ↔ neutral, neutral ↔ base). Analyze various reversibility combinations. To analyze the pH sensitivity of the sample in the artificial sweat environment the preparation of acidic (pH 4.4) and basic (pH 8) sweat that was prepared by following reported procedure[34]. To analyze its efficiency the sample was dipped inside the prepared sweat solution for one minute and changes were studied accordingly.

4.4 Stability of sensor to real conditions:

To investigate the durability of the fabric sensor against the washing and rubbing considering its application. Washing fastness was performed using non-ionic soap solution of 2 gpl at 60°C for 30 minutes in the Laundrometer. Dry and wet rub fastness of dyed wool fabric samples were tested using a crock meter as per standard IS 766:1988 (Reaffirmed 2004) based on ISO 105-X12:2001 by mounting the yarn/fabric on panel and giving ten strokes for both dry and wet rub fastness tests.

Conclusion:

In conclusion, this study introduces a sweat pH detection patch made from wool and HPTS (Pyranine) via conventional dyeing as fabrication protocol. The sensor detects sweat pH across a wide range under visible and UV light, with high sensitivity and real-time response. It can collect and detect pH levels simultaneously without extra accessories, reducing complexity and waste. Being wool-based, it's biodegradable, reusable, and compatible with the body, making it promising for development of eco-friendly health monitoring applications.

Conflicts of interest

There is no conflict of interest declared

Supporting Information

Supporting Information is available.

Acknowledgements

The authors are thankful to the Science and Engineering Research Board (SERB) Sanction No-ECR/2017/001204, Innovation in Science Pursuit for Inspired Research (INSPIRE) Sanction No-DST/INSPIRE/04/2015/001337, Department of Science and Technology (DST), Govt. of India, National Technical Textiles Mission (NTTM-Edu-23-00052) and All-India Council for Technical Education, India (ADF-S2021167) for the financial support. The author would also like to express gratitude to Neelikon Food Dyes and Chemicals Limited, India, for generously providing the chemicals used in this research.

References

1. 1997-stern-diagnosis of cystic fibrosis.
2. A. T. Hastie, S. T. Hingley, F. Kueppers, M. L. Higgins, C. S. Tannenbaum and G. Weinbaum2, *Protease Production by Pseudomonas aeruginosa Isolates from Patients with Cystic Fibrosis*, 1983, vol. 40.
3. J.-H. Ha, Y. Jeong, J. Ahn, S. Hwang, S. Jeon, D. Kim, J. Ko, B. Kang, Y. Jung, J. Choi, H. Han, J. Gu, S. Cho, H. Kim, M. Bok, S. A. Park, J.-H. Jeong and I. Park, *Mater Horiz*, DOI:10.1039/d3mh00340j.
4. L. Rittié, D. L. Sachs, J. S. Orringer, J. J. Voorhees and G. J. Fisher, *American Journal of Pathology*, 2013, **182**, 163–171.

5. J. Diao, J. Liu, S. Wang, M. Chang, X. Wang, B. Guo, Q. Yu, F. Yan, Y. Su and Y. Wang, *Cell Death Dis*, DOI:10.1038/s41419-019-1485-5.
6. L. A. Nattkemper, H. G. Lee, R. Valdes-Rodriguez, N. K. Mollanazar, K. M. Sanders and G. Yosipovitch, *Cholinergic induction of perspiration attenuates non-histaminergic pruritus in the skin of atopic dermatitis subjects and healthy controls Sweat and itch in atopic dermatitis and healthy controls*,
7. J. Moyer, D. Wilson, I. Finkelshtein, B. Wong and R. Potts, *Diabetes Technol Ther*, 2012, **14**, 398–402.
8. H. Nose, G. W. Mack, X. Shi, E. R. NADEL John B Pierce, W. Mack, X. S-ii and E. R. Nadel, *Shift in body fluid compartments after dehydration in humans*, 1988.
9. P. Pilardeau, J. Vaysse, M. Garnier, M. Joublin and L. Valeri, *Br J Sports Med*, 1979, **13**, 118–121.
10. K. Matsubayashi, M. Suzuki, E. Tamiya and I. Karube, *Analysis of metabolites in sweat as a measure of physical condition the increasing desire to naturally enhance the performance of sportsmen and athletes through*, 1994, vol. 289.
11. R. C. Klesges, K. D. Ward, M. L. Shelton, W. B. Applegate, E. D. Cantler, G. M. A. Palmieri, K. Harmon and J. Davis, *Changes in Bone Mineral Content in Male Athletes Mechanisms of Action and Intervention Effects*.
12. M. F. Bergeron, *N PHYSIOLOGY: Training to play Heat cramps: fluid and electrolyte challenges during tennis in the heat*.
13. K. Y. Yung, A. J. S. Hewitt, N. P. Hunter, F. V. Bright and G. A. Baker, *Chemical Communications*, 2011, **47**, 4775–4777.
14. J. Cui, Y. Li, D. Chen, T. G. Zhan and K. da Zhang, *Adv Funct Mater*, 2020, 30.
15. V. F. Curto, C. Fay, S. Coyle, R. Byrne, C. O'Toole, C. Barry, S. Hughes, N. Moyna, D. Diamond and F. Benito-Lopez, *Sens Actuators B Chem*, 2012, **171–172**, 1327–1334.
16. H. Y. Y. Nyein, W. Gao, Z. Shahpar, S. Emaminejad, S. Challa, K. Chen, H. M. Fahad, L. C. Tai, H. Ota, R. W. Davis and A. Javey, *ACS Nano*, 2016, **10**, 7216–7224.
17. J. Park, D. I. Cha, Y. Jeong, H. Park, J. Lee, T. W. Kang, H. K. Lim and I. Park, *Advanced Science*, DOI:10.1002/advs.202100725.
18. N. Padmanathan, H. Shao and K. M. Razeeb, *ACS Appl Mater Interfaces*, 2018, **10**, 8599–8610.

19. N. Promphet, P. Rattanawaleedirojn, K. Siralertmukul, N. Soatthiyanon, P. Potiyaraj, C. Thanawattano, J. P. Hinestroza and N. Rodthongkum, *Talanta*, 2019, **192**, 424–430.
20. L. Wang, L. Wang, Y. Zhang, J. Pan, S. Li, X. Sun, B. Zhang and H. Peng, *Adv Funct Mater*, DOI:10.1002/adfm.201804456.
21. M. Y. Choi, M. Lee, J. H. Kim, S. Kim, J. Choi, J. H. So and H. J. Koo, *Journal of Industrial Textiles*, 2022, **51**, 441S-457S.
22. F. T. Giachet, C. Vineis, D. O. Sanchez Ramirez, R. A. Carletto, A. Varesano and G. Mazzuchetti, *Fibers and Polymers*, 2017, **18**, 720–730.
23. L. Possanzini, F. Decataldo, F. Mariani, I. Gualandi, M. Tessarolo, E. Scavetta and B. Fraboni, *Sci Rep*, DOI:10.1038/s41598-020-74337-w
24. S. Ulrich, A. Osypova, G. Panzarasa, R. M. Rossi, N. Bruns and L. F. Boesel, *Macromol Rapid Commun*, DOI:10.1002/marc.201900360.
25. K. Kano and J. H. Fendler, *PYRANINE AS A SENSITIVE pH PROBE FOR LIPOSOME INTERIORS AND SURFACES pH GRADIENTS ACROSS PHOSPHOLIPID VESICLES*, 1978, vol. 509.
26. R. S. Bhosale, G. V. Shitre, R. Kumar, D. O. Biradar, S. V. Bhosale, R. Narayan and S. V. Bhosale, *Sens Actuators B Chem*, 2017, **241**, 1270–1275.
27. N. Sekar, in *Handbook of Textile and Industrial Dyeing: Principles, Processes and Types of Dyes*, Elsevier Inc., 2011, vol. 1, pp. 486–514.
28. B. Wei, Q. Y. Chen, G. Chen, R. C. Tang and J. Zhang, *J Chem*, , DOI:10.1155/2013/546839.
29. Y. Avnir and Y. Barenholz, *Anal Biochem*, 2005, **347**, 34–41.
30. W. Heo, N. Uddin, J. W. Park, Y. M. Rhee, C. H. Choi and T. Joo, *Physical Chemistry Chemical Physics*, 2017, **19**, 18243–18251.
31. F. Han, W. Liu and C. Fang, Chem Phys, 2013, 422, 204–219.
32. A. Grandjean, J. L. Pérez Lustres and G. Jung, ChemPhotoChem, 2021, 5, 1094–1105.
33. R. Nandi and N. Amdursky, Acc Chem Res, 2022, 55, 2728–2739.
34. R. Chen, J. qu, D. Yang and J. he, Textile Research Journal, 2014, 84, 772–782